Acta Biomaterialia 168 (2023) 264–276

Contents lists available at ScienceDirect

Acta Biomaterialia

journal homepage: www.elsevier.com/locate/actbio

Full length article

Multimodal and multiscale characterization reveals how tendon structure and mechanical response are altered by reduced loading

Maria Pierantoni[a,1,*], Isabella Silva Barreto[a,1], Malin Hammerman[a,b], Vladimir Novak[c], Ana Diaz[c], Jonas Engqvist[d], Pernilla Eliasson[b,e], Hanna Isaksson[a]

[a] Department of Biomedical Engineering, Lund University, Box 118, 221 00 Lund, Sweden
[b] Department of Biomedical and Clinical Sciences, Linköping University, 581 83 Linköping, Sweden
[c] Paul Scherrer Institute, 5232 Villigen PSI, Switzerland
[d] Department of Solid Mechanics, Lund University, Box 118, 221 00 Lund, Sweden
[e] Department of Orthopaedics, Sahlgrenska University Hospital, Gothenburg, Sweden

ARTICLE INFO

Article history:
Received 18 April 2023
Revised 30 June 2023
Accepted 14 July 2023
Available online 20 July 2023

Keywords:
Collagen fibers
Mechanobiology
Synchrotron imaging
Scattering
Tomography
3D orientations

ABSTRACT

Tendons are collagen-based connective tissues where the composition, structure and mechanics respond and adapt to the local mechanical environment. Adaptation to prolonged inactivity can result in stiffer tendons that are more prone to injury. However, the complex relation between reduced loading, structure, and mechanical performance is still not fully understood. This study combines mechanical testing with high-resolution synchrotron X-ray imaging, scattering techniques and histology to elucidate how reduced loading affects the structural properties and mechanical response of rat Achilles tendons on multiple length scales. The results show that reduced in vivo loading leads to more crimped and less organized fibers and this structural inhomogeneity could be the reason for the altered mechanical response. Unloading also seems to change the fibril response, possibly by altering the strain partitioning between hierarchical levels, and to reduce cell density. This study elucidates the relation between in vivo loading, the Achilles tendon nano-, meso–structure and mechanical response. The results provide fundamental insights into the mechanoregulatory mechanisms guiding the intricate biomechanics, tissue structural organization, and performance of complex collagen-based tissues.

Statement of significance

Achilles tendon properties allow a dynamic interaction between muscles and tendon and influence force transmission during locomotion. Lack of physiological loading can have dramatic effects on tendon structure and mechanical properties. We have combined the use of cutting-edge high-resolution synchrotron techniques with mechanical testing to show how reduced loading affects the tendon on multiple hierarchical levels (from nanoscale up to whole organ) clarifying the relation between structural changes and mechanical performance. Our findings set the first step to address a significant healthcare challenge, such as the design of tailored rehabilitations that take into consideration structural changes after tendon immobilization.

1. Introduction

Collagen is the major component of all connective tissues and represents approximately one quarter of the total dry weight of mammals [1]. One of the functions of connective tissues is to transmit forces. To perform the task effectively, collagen must be disposed along the direction of mechanical loads, such as in tendons [2,3]. The structure of tendons is complex and ranges over multiple hierarchical levels. From the nanoscale, the collagen molecules arrange into fibrils, which align together to form collagen fibers, which can be comprised in bundles [4]. This structural arrangement leads to an anisotropic tissue with high tensile strength, flexibility, and damping properties [5–7].

* Corresponding author at: Department of Biomedical Engineering, Lund University/LTH, Box 118, 221 00 Lund, Sweden.
E-mail address: maria.pierantoni@bme.lth.se (M. Pierantoni).
[1] Maria Pierantoni and Isabella Silva Barreto are equal contributors.

https://doi.org/10.1016/j.actbio.2023.07.021

Human studies and animal models have shown that mechanical forces are fundamental to maintain tendon health [8,9]. Reduced mechanical stimuli can lead to a reduced cross-sectional area of the tendon, changes in structural organization and impaired tendon biomechanical properties [4,10]. Mechanical loading can also affect collagen production, and it can e.g. be increased by exercise and decreased by reduced loading [8,11,12]. Although, there is a range in which loading is beneficial to the tendon, both insufficient and excessive loading can be detrimental [13,14]. In particular, in Achilles tendons the stiffness was reported to decrease by ∼28% in patients after 20 days of bed rest [15], ∼58% after 90 days of simulated microgravity [16], and ∼59% after a period of paralysis [17]. Furthermore, athletes returning to heavy training quickly after a period of inactivity face a high risk of tendon rupture [18], as well as people living mostly a sedentary lifestyle in later life while intermittently engaging in recreational sports [19,20]. Thus, the adaptation of tendons in response to prolonged inactivity, may directly affect the incidence of rupture. However, the refined details of how tendon microstructure, mechanical performance, and collagen production are affected by loading are not known [21]. Therefore, a detailed investigation of the tendon hierarchical organization is important to improve our understanding of the biochemical, biomechanical, and structural adaptation of Achilles tendons in relation to physical activity and lack thereof.

In this study we have investigated the rat Achilles tendon which is the largest tendon in the human body and operates as a bridge for muscular force transmission by connecting the calf muscle to the heel bone [22,23]. Achilles tendons are formed of 3 distinct sub-tendons that connect to the soleus (SOL), and to the lateral and medial gastrocnemius muscles (LG and MG, respectively) [24]. Earlier studies that investigated the microstructure of Achilles tendons primarily focused on 2D microscopy in combination with chemical staining and immunohistochemistry [25,26]. In this study, we extend our current understanding of the relation between micro- and nano- structure and the mechanics of Achilles tendons by 3D high-resolution visualization using synchrotron X-ray imaging and scattering techniques, such as phase-contrast enhanced synchrotron micro-tomography (SR-PhC-μCT) and small-angle X-ray scattering (SAXS) (Fig. 1). SR-PhC-μCT is suitable for studying the complex 3D microstructure of soft tissues, including tendons [27–29]. At the nanoscale, SAXS can be used to probe the periodically arranged tropocollagen molecules inside the fibrils, and provide information about structural properties at the nanoscale [10,30,31]. SAXS, in combination with in situ mechanical loading, provides information on collagen fibril strain, strain heterogeneity, fibril organization, and degree of orientation in response to loading [32–36]. By performing SR-PhC-μCT, histology, SAXS and mechanical testing we have used a multimodal approach to investigate microstructural organization, collagen fibril structural response to in situ loading, biomechanical properties, and extracellular matrix protein content of rat Achilles tendons which were either unloaded (UL) by Botox injections in combination with ankle immobilization or were normally loaded (full loading, FL) through free cage activity. With this data, we contribute to closing existing gaps between the mechanobiological adaptation of the whole-tendon mechanics and micro- and nanoscale structural response, strengthening our understanding of how mechanical stimulation, structure, and performance are linked. We hypothesized that reduced mechanical stimulation affects nano- and micro-organization of collagen, which impairs the mechanical response of Achilles tendons.

2. Materials and methods

2.1. Animal model

Female Sprague-Dawley rats (specific pathogen free (SPF), age 10–12 weeks, from Janvier, Le Genest-Saint-Isle, France, $n = 55$) were used to characterize the effect of in vivo loading (Table 1). The rats were kept two per cage with a light-dark cycle of 12 h, and in controlled humidity (55%) and temperature (22 °C). Food was provided ad libitum. The rats were randomly divided into two groups with different in vivo loading scenarios: 1) full loading (FL) through free cage activity and 2) unloading (UL) through Botox injections combined with joint fixation using a steel-orthosis [37]. Botox (3U, Botulinum toxin, Allergan, Irvine, CA) was injected during sedation in the right calf muscle (soleus, gastrocnemius lateralis and medialis, 1U (0.02 ml) / muscle) before the start of

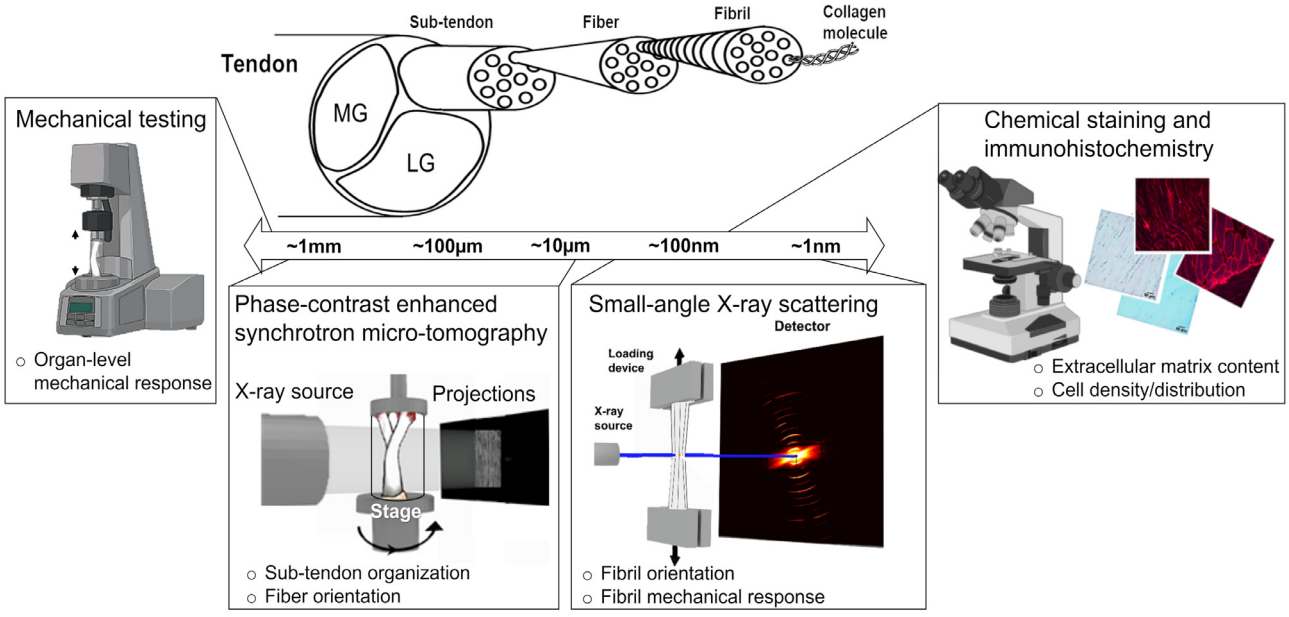

Fig. 1. Outline of the multimodal and multiscale methodology to investigate the mechanobiological adaptation of the Achilles tendon tissue. The hierarchical structural organization of rat Achilles tendons, exposed to full loading (FL) or unloading (UL) in vivo, were studied at different length scales by phase-contrast enhanced synchrotron micro-tomography, small-angle X-ray scattering in combination with mechanical testing, and by histology. The mechanical response at the whole organ level was also tested.

Table 1
Experimental setup and number of rats/tendons assessed with the different characterization techniques.

Experiment	Fully loaded (FL)	Unloaded (UL)
Microstructural characterization (SR-PhC-μCT)	7	7
Collagen response to loading (in situ SAXS)		
• Ramp to failure	6	4
• Stress relaxation	4	4
Tissue mechanical response (*ex situ* mechanical testing)	9	10
Extracellular matrix and cell content (histology)	5	6

the experiment, to induce plantar flexor muscle paralysis. The rats were sacrificed after 4 weeks, based on previous studies showing that Botox injections in the rat calf muscle remain effective during this time [10,38,39]. After the rats had been sacrificed, the right Achilles tendon was dissected free from the skin and harvested together with the calcaneus and calf muscles. The tendons were then stored at −20° until measurements, which should not cause any detrimental effect on the tissue mechanical properties [40–42]. The experiments adhered to the institutional guidelines for care and treatment of laboratory animals. The study was approved by the Regional Ethics Committee for animal experiments in Linköping, Sweden (Jordbruksverket, ID1424), and was performed in compliance with the ARRIVE Guidelines.

2.2. Phase contrast enhanced synchrotron X-ray tomography (SR-PhC-μCT)

The imaging was performed at the X02DA TOMCAT beamline at the Swiss Light Source (SLS), Paul Scherrer Institute (Villigen, Switzerland) [43]. The images were acquired using a high numerical aperture microscope setup, 4x magnification, field of view (FOV) of 4.2 × 3.5 mm and a voxel size of 1.63×1.63×1.63 µm^3. A propagation distance of 150 mm was chosen, and the X-ray energy was set at 15 keV. 2001 projections were acquired over 180° of continuous rotation. The exposure time was 33 ms resulting in about 90 s scans. Image analysis was performed in MATLAB, volume renderings and visualizations were performed in ImageJ and Dragonfly (v 4.1, ORS software) [44,45]. The orientation distribution of collagen fibers in tendons was determined in 3D by performing a structure tensor analysis, adapting a MATLAB script based on Saxena et al. and on Krause et al. [46,47]. For more information about the SR-PhC-μCT experiment and data analysis see Supporting information, Method S1 and Figure S1.

2.3. In situ *loading combined with small-angle X-ray scattering (SAXS)*

SAXS measurements were conducted at the coherent small-angle X-ray scattering beamline (cSAXS) at the Swiss Light Source (SLS), Paul Scherrer Institut (PSI), Switzerland using a similar protocol as previously developed by the authors [48]. Measurements were conducted using a beam energy of 12.4 keV (wavelength λ of ~1 Å), an exposure time of 50 ms, a beam size of 150×125 μm^2 and a sample-detector distance of ~7.14 m, enabling data acquisition in the q-range of ~0.02–1.45 nm^{-1}. SAXS measurements were acquired from one spot in the center of the tendon.

SAXS measurements can be performed during in situ loading [30,32,33,36], i.e. by mechanically loading the whole tendon while simultaneously acquiring scattering data. This allows to determine collagen mechanical response at the nanoscale. For in situ mechanical tests, tendons were first preloaded to 1 N and then loaded at 5 mm/min, by either ramp to failure, or stress relaxation (Table 1). During ramp to failure, SAXS measurements were acquired at intervals of 1.2 s. During stress relaxation, the tendons were displaced for two steps of 0.3 mm, followed by 300 s relaxation. For each step, 10 SAXS measurements at 1.2 s intervals followed by 12 measurements at 25 s intervals were acquired. With this setup, the results are not significantly affected by radiation damage to the sample, as previously described [48]. Analysis of the 2D scattering patterns was performed using in-house codes in MATLAB [31] following our previously described protocols [48]. For more information about SAXS experiment and data analysis see Supporting information, Method S2, Figure S2 and Table S1 A.

2.4. Ex situ *mechanical testing*

To elucidate how the tendon mechanical response is affected by unloading at the organ scale, mechanical tests were performed in the lab on FL and UL tendons (without concurrent scattering as in 2.3, therefore called ex situ).

Rat tendons (physiological data are reported in Supporting information table S1 B) were mechanically tested using an Instron 8511 load frame (Instron, USA) connected to an Interface SMT1-250 N load cell (Interface, USA), and controlled by MTS TestStarII (MTS Systems, USA). Tendons were first preloaded to 1N and then loaded in tension (Supporting information, Figure S2 B). The testing protocol consisted of three loading regimes: a) cyclic loading: 10 cycles of 6% strain at 0.1 mm/s followed by 300 s of rest; b) 2 steps of stress relaxation: 8% and 16% strain at 1 mm/s, each followed by 500 s relaxation time; and c) ramp to failure at 1 mm/s. For more information about the testing protocol and data analysis see Supporting information, Method S3, Table S1 B and Figure S3.

2.5. Histology

Rat tendons were embedded in OCT, snap-frozen, sectioned longitudinally (7 µm thickness), hydrated in PBTD (PBS containing 0.1% Tween20 and 1% DMSO), and fixed in 4% formaldehyde. Sections were stained with primary polyclonal antibodies from rabbit against collagen type I / collagen type III / or elastin followed by a goat anti-rabbit IgG secondary antibody, and lastly counterstained with DAPI. Stained sections were examined using a Leica DMi8 microscope. Nuclear fast red & alcian blue staining was also used (to visualize proteoglycans), as well as hematoxylin & eosin. For more information about histology and data analysis see Supporting information, Method S4 and Figure S4.

2.6. Statistics

Some of our data was not normally distributed. Therefore, a non-parametric Mann-Whitney *U* test (unpaired, 5% significance level) was performed to test for significant differences between FL and UL Achilles tendons. A Wilcoxon signed rank test (paired, 5% significance level) was performed to test for significant differences between different locations within the same tendon (MG, LG and SOL).

3. Results

3.1. Achilles tendon collagen fibers are more crimped when loading is reduced

SR-PhC-μCT provided a comprehensive insight into the complex 3D internal collagen fiber microstructure (Fig. 2 and video S1), where UL tendons were more crimped compared to FL tendons. The fiber orientation analysis (based on the use of 3D structural tensors) showed that azimuth and elevation angle distributions for UL fibers have tails that were not present in the angle distributions for fibers from FL tendons (Fig. 2B arrows). The mean full width at half maximum (FWHM) of both azimuth and elevation angles indicates a wider orientation spread in fibers from UL compared to FL tendons (azimuth spread UL: **77**° ± 49° vs FL: **48**° ± 22°, elevation spread UL: **22**° ± 7° vs FL: **17**° ± 6°).

The bivariate histograms, obtained by combining azimuth and elevation angle distributions, were also significantly ($p = 0.007$) wider in UL compared to FL tendons (**0.4** ± 0.2 vs **0.2** ± 0.6), which indicates a wider range of orientations in UL tendons (Fig. 2C and D). However, UL and FL tendon bivariate histograms had similar cross-sections at high angle occurrence (area at 75% of the total counts, Fig. 2C), which shows that the longitudinal axis of the fibers were mostly oriented along the main tendon axis in both UL and FL tendons. Even so, the lower part of the bivariate histograms was wider for fibers in UL compared to FL tendons (area at 25% of the total counts, Fig. 2C), which indicates local orientation heterogeneities. Thus, in many small regions of UL tendons, fibers were more crimped and diverged from the tendon main axes (Fig. 2A and video S1). The differences in the shape of bivariate histograms were quantified as skewness and kurtosis, showing significant differences between UL and FL tendons (Fig. 2D). Furthermore, the fibers were less densely packed in UL tendons (Fig. 2D, UL fiber density: **78–88**% vs FL: **82–92**%).

When testing for local variations in fiber orientation, fibers in UL tendons were in general less homogeneously oriented than fibers in FL tendons. However, local differences (e.g. due to crimping) and standard deviations were larger in UL tendons (Supporting information Figure S5).

The fiber orientation analysis for different sub-tendons was performed close to the musculo-tendinous junction. The medial and lateral gastrocnemius sub-tendons (MG and LG) were characterized by a similar level of fiber organization, while the soleus subtendon (SOL) was significantly less organized, irrespective of loading regimen (Fig. 2F and Supporting information Fig. S6). It should however be noticed that fibers close to the musculo-tendinous junction were less organized and more crimped compared to the mid-tendon region for all the three sub-tendons and both loading regimes (Fig. 2E and F, Supporting information Fig. S6).

3.2. Fibrils can be oriented along one main axis or two axes depending on the orientation of the sub-tendons

Small-angle X-ray scattering (SAXS) provided further understanding of the structural organization of collagen at the fibril level. Two types of scattering patterns were detected from the SAXS data, either a single population of fibrils (Fig. 3A i) or two sub-populations with almost equal number of fibrils in each subpopulation (Fig. 3A ii). The orientations of the two sub-populations were clearly distinct and comparable to the one observed at the tendon level, between the MG and LG main axes (Fig. 3B). The two sub-populations were more commonly seen in UL than FL tendons (UL **4** tendons vs FL **1** tendon). When only one population was present, the most aligned fibrils strained more during the in situ loading compared to the average of the whole population. Whereas, when two sub-populations were observed, one sub-population strained more and the other less than the average population (Fig. 3, i and ii, right).

3.3. Mechanical response in fibrils is delayed in unloaded tendons

During SAXS with concurrent tensile loading (in situ) UL tendons displaced more than FL in a ramp to failure (Supporting information Fig. S7A). However, there was no difference in stiffness (UL: **41** ± 14 N/mm; FL: **38** ± 15 N/mm) and similar maximum tissue stress was reached, as well as tissue stress at maximum D-spacing and tissue stress at yield (Supporting information Fig. S7A ii). The initial fibril strain was less in UL than in FL tendons (Fig. 4A i), whereas the tissue strains at the point of maximum D-spacing and yield point were similar, indicating that the fibrils failed close to tissue yield in both cases (Supporting information Fig. S7A iii). However, in some of the tendons, the fibrils may have failed prior to tissue yield as the tissue strain at yield were larger than at maximum D-spacing. The initial D-spacing was the same for UL and FL tendons, and the two groups reached similar maximum D-spacing values and maintained similar values at yield (Fig. 4A iv). No clear differences in intrafibrillar disorder were observed (Fig. 4A ii and v). The relative fibril strain heterogeneity in UL tendons was initially smaller, but then at tissue yield became slightly larger than in FL tendons (Fig. 4A iii and vi).

During in situ SAXS, in a stress relaxation configuration, UL tendons were characterized by higher stress relaxation ratio during the first step (1st step UL: **0.59** ± 0.22, FL: **0.38** ± 0.12; 2nd step UL: 0.**38** ± 0.10 MPa, FL: **0.41** ± 0.09 MPa, Supporting information Figure S7B iii) and reached lower stresses for the same strain compared to FL (1st step UL: **1.2** ± 0.5 MPa, FL: **3.9** ± 2.3 MPa; 2nd step UL: **3** ± 1 MPa, FL: **4** ± 2 MPa, Supporting information Figure S7B i-ii). Fibrils in UL tendons generally strained less than fibrils in FL tendons (1st step UL: **0.16** ± 0.07%, FL: **0.6** ± 0.5%; 2nd step UL: **0.35** ± 0.06%, FL: **0.8** ± 0.5%, Fig. 4B i and ii), as observed during ramp to failure tests. During the second step of stress relaxation, UL tendons exhibited slightly larger fibril strain relaxation ratios compared to FL tendons (2nd step UL: **0.55** ± 0.08 s, FL: **0.3** ± 0.2 s, Fig. 4B iii), and had faster fibril relaxation times (1st step UL: **29** ± 13 s, FL: **57** ± 42 s; 2nd step UL: **22** ± 13 s, FL: **42** ± 28 s, Fig. 4B iv).

Generally, fibril stress relaxation was 10–20% slower than tissue stress relaxation (Fig. 4B iv and Supporting information, Figure S7B iv), irrespective of loading regimen. The ratios of tissue to fibril level relaxation times were similar between UL and FL tendons (1*st* step UL: **0.9** ± 0.4, FL: **0.8** ± 0.5; 2*nd* step UL: **0.9** ± 0.7, FL: **0.9** ± 0.5).

3.4. Unloading impairs the mechanical response of the whole tendon

Achilles tendons were mechanically tested by cyclic loading, followed by two steps of stress relaxation, and lastly ramp to failure. UL tendons were characterized by larger standard deviations compared to FL tendons. During cyclic loading at 6% strain (Fig. 5A), UL and FL tendons reached similar stress, and had similar elastic moduli (Fig. 5A ii and iii). However, UL tendons had significantly longer toe regions during the first cycle (UL: **0.028**±0.008 vs FL: **0.02**±0.11, $p = 0.02$, Fig. 5A iv). UL tendons exhibited slightly longer cyclic periods, which resulted in an accumulated time delay with increasing cycles, compared to FL tendons (Fig. 5A i-ii). In the second step of stress relaxation (Fig. 5B), UL tendons reached lower stress than FL tendons (UL: **18**±11 N/m^2 vs FL: **29**±7 N/m^2, $p = 0.013$), higher stress relaxation ratio (UL: **0.7** ± 0.1 vs FL: **0.50**±0.06, $p<0.0001$), and faster relaxation times (UL: **16**±5 s vs FL: **23**±2 s, $p<0.0001$). The elastic modulus of UL tendons was slightly lower compared to FL tendons during the second step, but the difference was not significant (UL: **273**±131 MPa vs FL:

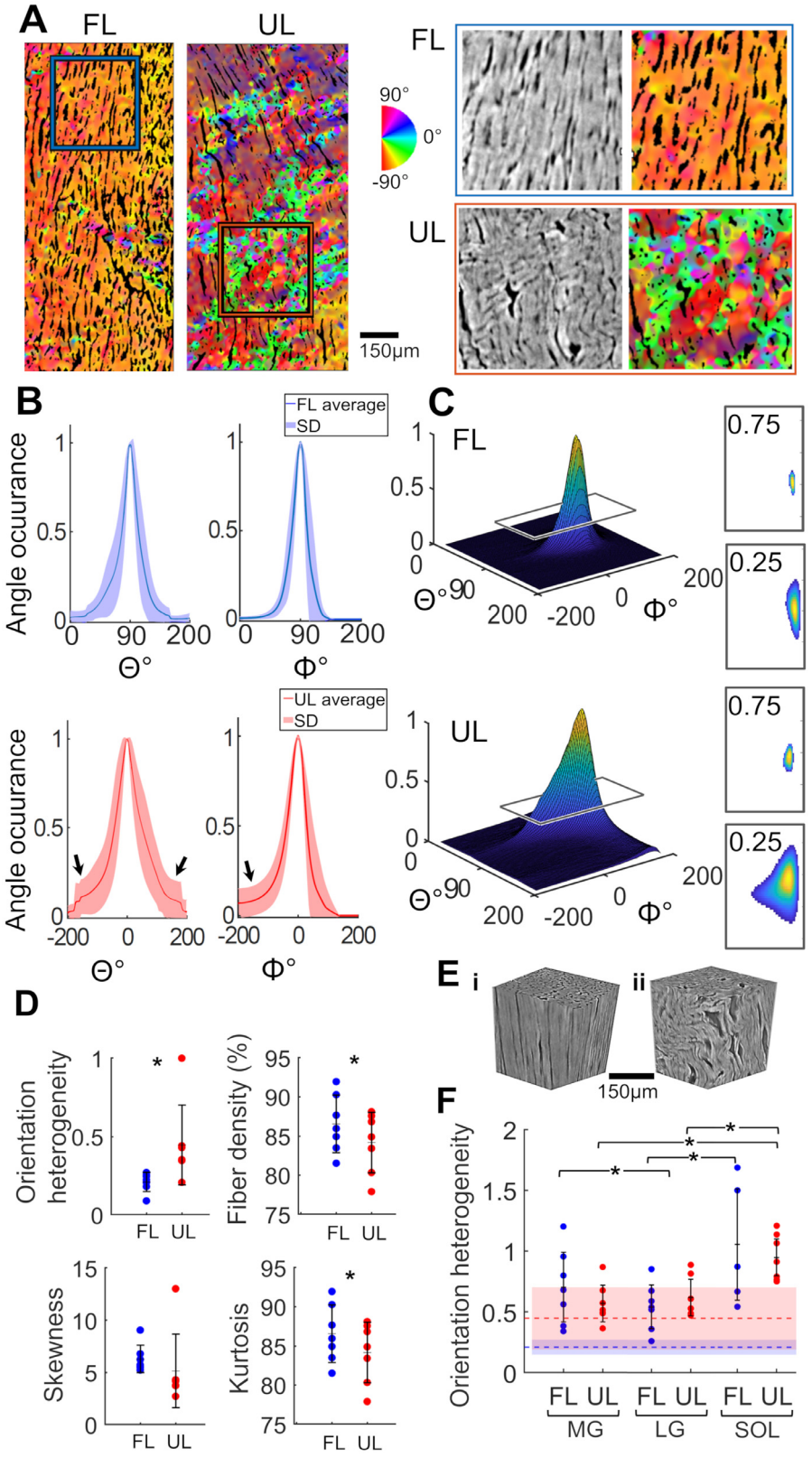

Fig. 2. Fiber organization in the center of fully loaded (FL) and unloaded (UL) tendons. FL fibers are well orientated, whereas UL fibers are more crimped. A) Colormaps showing fiber organization for FL and UL tendons in the center of the tendon tissue, the magnifications show well orientated fibers in FL and crimped fibers in UL tendons. B) Mean and standard deviation of azimuth (θ) and elevation (Φ) angles for FL (top, in blue) and UL tendons (bottom, in red). C) Bivariate histograms showing 3D fiber orientation distribution for FL (top) and UL (bottom) tendons. On the right, cross sections are shown at 75% and 25% of the curves as indicated by the cutting planes. D) Orientation heterogeneity, fiber density, skewness (describing the symmetry of the data distribution) and kurtosis (describing the "tailedness" of the data distribution). Individual data points (dots) and mean ± standard deviation (black lines) are shown. Statistically significant differences between UL (red) and FL (blue) tendons (* $p< 0.05$) are indicated. E) SR-PhC-μCT volume renderings showing fibers from the same FL tendon; i) in the center, and ii) at in upper region of the tendon (close to the muscles). F) Fiber orientation heterogeneity in the 3 sub-tendons (medial, MG, and lateral gastrocnemius, LG, and soleus, SOL, sub-tendons,) compared to mean values and standard deviations for the center of the tendon tissue (the results are indicated by the dashed lines for the mean values, and by shadowed areas indicating the standard deviations). UL are in red and FL in blue. Significant differences are indicated (* $p< 0.05$).

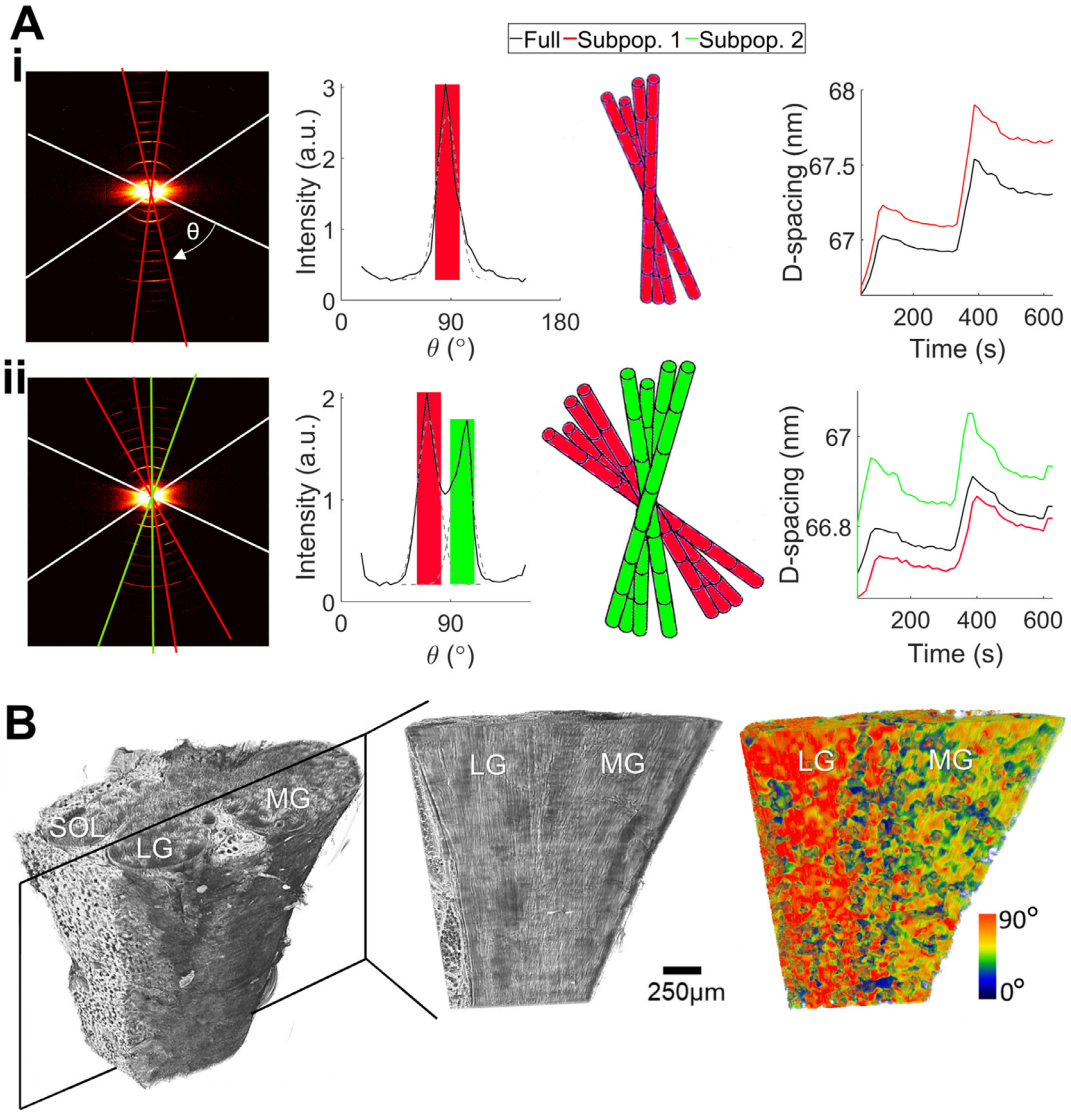

Fig. 3. Nanoscale fibril orientation and its relation to sub-tendon macro arrangement. A) Left: SAXS scattering patterns of a representative tendon with one population of fibrils (i) compared to a tendon with two sub-populations (ii). Middle: Angularly integrated curves (θ) of SAXS patterns and schematic illustrations of fibril orientation. Right: The response in D-spacing of fibril sub-populations azimuthally integrated within their respective main orientation ± 10° (indicated by the correspondingly colored lines on the scattering patterns) compared to the overall response of the full fibril population (black lines), azimuthally integrated within the average orientation ± 60° (indicated by the white lines on the scattering pattern). B) SR-PhC-μCT renderings in gray scale and colormap (0°–90°) showing differences between the main orientation of MG (red-orange) and LG (yellow-green) sub-tendons.

375±86 MPa, Fig. 5B ii). During ramp to failure, both maximum stress and elastic modulus were significantly lower in UL tendons compared to FL tendons (maximum stress UL: **30**±20 N/m^2 vs FL: **69**±14 N/m^2, $p = 0.012$, and elastic modulus UL: **401**±199 MPa vs FL: **728**±234 MPa, $p = 0.005$, Fig. 5C).

3.5. Cell number decreases in unloaded tendons whereas content of extracellular matrix proteins is unchanged

Immunohistochemical staining for collagen type I, collagen type III, and elastin showed no statistical difference in the mean intensity measurements between UL and FL tendons. However, a slight reduction in elastin content may occur (Fig. 6A and B ii-iv). Image quantification of cell nuclei staining (DAPI) showed that cell number density was significantly lower in UL compared to FL tendons (UL: **0.93**±0.06, vs FL: **0.7** ± 0.2, $p = 0.017$), as shown by H&E staining (Supporting information, Figure S8A). Staining with alcain blue revealed no significant differences in proteoglycan content between the two groups (Supporting information, Figure S8B).

4. Discussion

This study presents an extensive multiscale investigation of the effect of reduced mechanical stimulation on collagen-based tissues, exemplified by the Achilles tendon. The complex hierarchical structure of the Achilles tendon was probed from the organ tissue-level, down to the nano-level of fibrils, using cutting-edge high-resolution synchrotron techniques. The results show that mechanical stimuli are fundamental to preserve Achilles tendon physiological microstructure required for an effective mechanical response.

It has previously been hypothesized that the mechanical properties of human tendons undergo considerable changes following extended disuse, which may be partly due to altered structure and composition [8,12,17]. Rat models represent a powerful tool to investigate the effect of unloading in the Achilles tendon [49]. In humans, Achilles tendons are usually examined only when injuries occur, whereas animal models enable us to investigate the tendon tissue under controlled conditions, even in the absence of injuries,

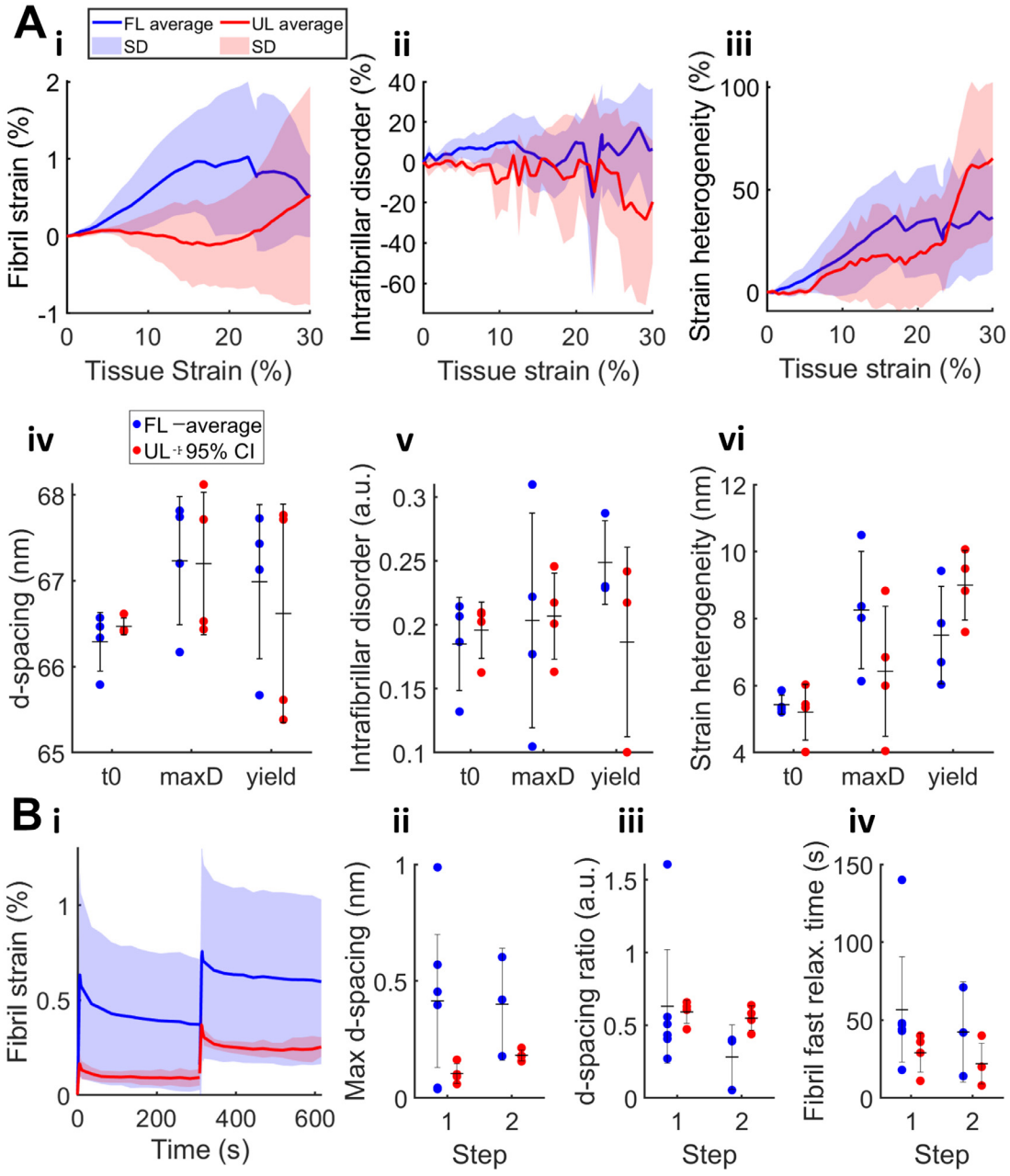

Fig. 4. Fibril response to in situ loading. A) Ramp to failure test comparing the average fibril behavior of FL (blue) and UL (red) tendons, showing: i) average relative response in fibril strain, ii) intrafibrillar disorder, iii) fibril strain heterogeneity, iv) absolute values of D-spacing, (v) intrafibrillar disorder, and (vi) strain heterogeneity at the start point of loading (t0), maximum D-spacing (maxD), and tissue yield (yield). B) Stress relaxation measurements comparing the average fibril behavior of FL and UL tendons, showing: i) average relative response in fibril strain, ii) maximum D-spacing as well as iii) fibril relaxation ratio and iv) fast relaxation times of the two steps. Plots display individual data points (dots), with mean ± standard deviation (black lines) for each group.

such as unloading of the Achilles tendon. Tendon biology and response to loading can vary among species, albeit certain fundamental mechanisms may be shared. The forces and strains applied to rat tendons may not accurately reflect the forces experienced by human tendons during daily activities, but they can provide a valuable starting point for understanding tendon response to loading. Thus, our results represent a first step for further research to design tailored approaches to help patients that undergo long periods of inactivity to regain tendon properties. In particular, our results show that 4 weeks of reduced loading on rat Achilles tendons reduced the microstructural fiber organization, which could explain the deferred mechanical response. This study shows that in vivo loading is crucial for tendons to maintain their mechanical properties. Reduced loading led to unorganized collagen structure and a decreased number of tenocytes, which can impair the Achilles tendon ability to withstand muscle forces making it more vulnerable to injuries [16].

4.1. Mechanical properties at tissue level are impaired by reduced loading

Previous studies have suggested that Achilles tendons adapt to reduced loading by showing a decrease in elastic modulus, and that the stiffness decrement may be directly correlated to the duration of unloading [15–17,50]. Our data confirm and expand these observations showing that UL tendons are characterized by a sig-

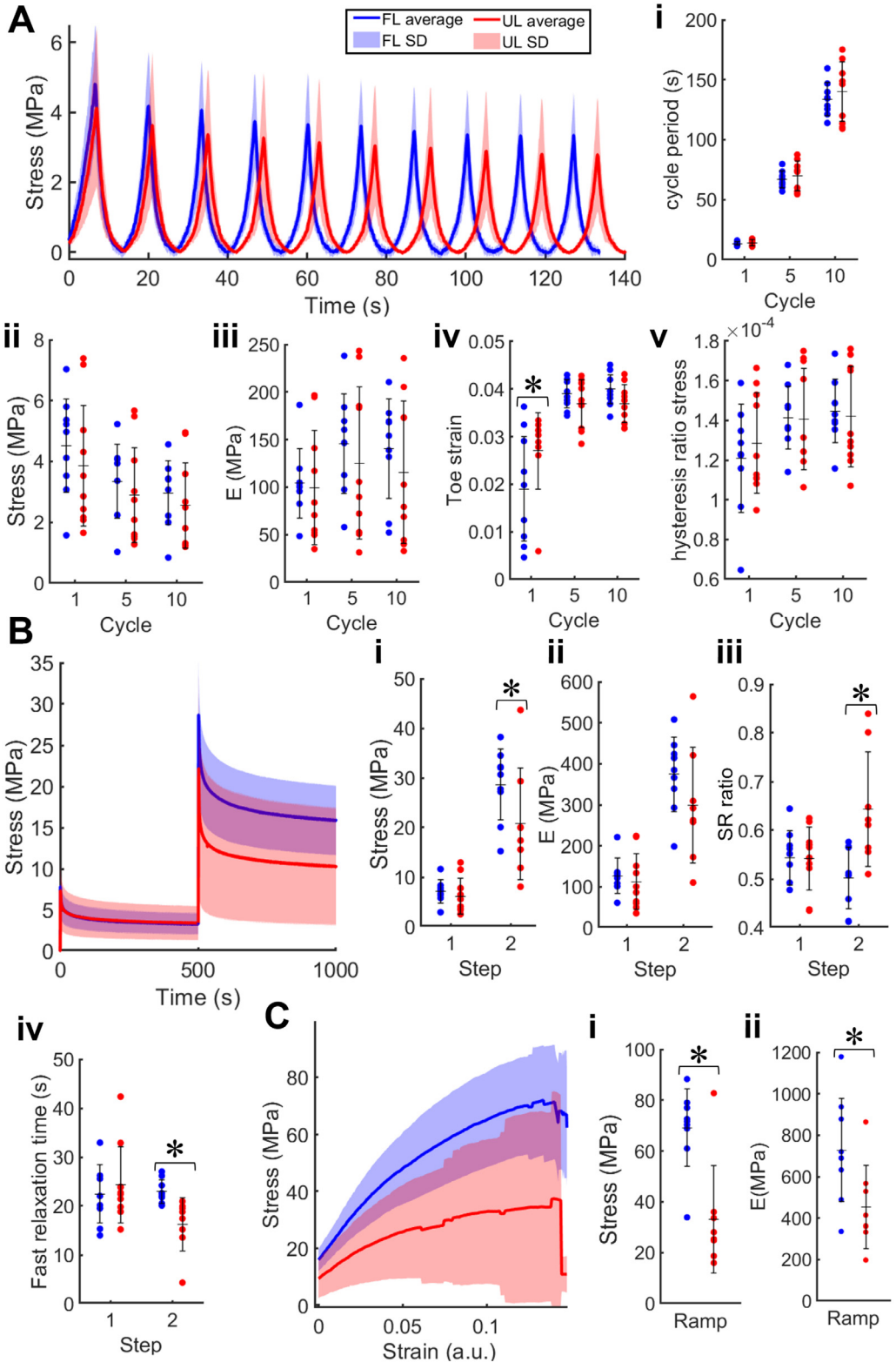

Fig. 5. Mechanical testing of fully loaded (FL) and unloaded (UL) tendons. A) Cyclic loading comparing the average behavior (normalized by cycle period) of FL (blue) and UL (red) tendons, showing: i) cyclic period (time at peak force), ii) stress at peak, iii) elastic modulus (E), iv) toe strain (extension of the toe region), and v) hysteresis ratio, for cycle 1, 5 and 10. B) Stress relaxation, comparing the average behavior of FL and UL tendons, showing: i) stress at peak, ii) elastic modulus (E) and iii) stress relaxation (SR) ratio, for the two steps. C) Ramp to failure, comparing the average behavior of FL and UL tendons, showing: i) stress at peak and ii) elastic modulus (E). In panels i-v, individual data points (dots) and mean ± standard deviation (black lines) are indicated for each group. Significant differences are indicated (* $p < 0.05$).

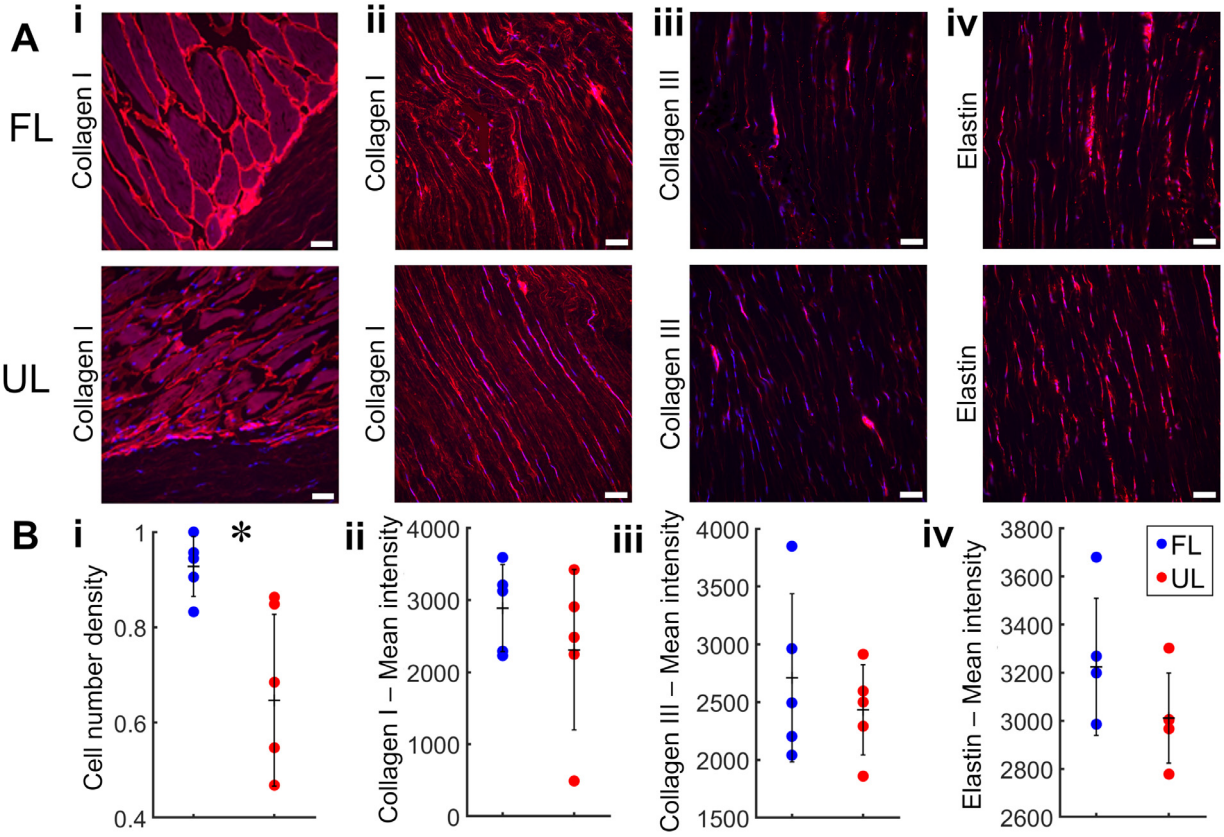

Fig. 6. Histological comparison of fully loaded (FL) and unloaded (UL) tendons by immunohistochemistry. A) Longitudinal sections of Achilles tendons stained with DAPI (cell nuclei: blue) and antibodies against three different extracellular matrix proteins as follow: i) Collagen I (red) showing the calf muscle, and ii) Collagen I (red), iii) Collagen III (red) and iv) elastin (red) showing tendon collagen fibers in the middle of the tendon tissue (scale bars: 50 μm). B) Quantification of cell number density (from DAPI staining, i) and quantifications of the mean intensity for collagen I, collagen III, and elastin (from antibodies staining, ii-iv). Graphs show individual data points (dots) and mean ± standard deviation (black lines) for FL (blue) and UL (red) tendons. Significant differences are indicated (* $p < 0.05$).

nificantly lower elastic modulus and increased stress relaxation ratio, compared to FL tendons. Furthermore, our results show that UL tendons relax faster than FL tendons, possibly due to microdamage which may already be occurring in UL tendons during the second step of stress relaxation (8–16% strain). This is further supported by the fact that 3 out of 10 UL tendons ruptured during the second step of stress relaxation whereas all FL tendons could withstand 16% strain.

4.2. Increased fiber crimping due to reduced loading and fibril mechanical response

Our results show that differences in mechanical performance between UL and FL tendons could originate from a combination of structural factors at different length scales. In particular, as crimp straightening occurs at low strains, increased crimping after unloading could explain the altered tendon mechanical response [51–53]. Increased fiber crimping would increase the time required for the fibers to straighten and orient homogeneously. This is further supported by the significantly longer toe region observed for UL tendons. A similar microstructure-mechanics relationship was hypothesized for another collagenous connective tissue, the lower dermis [54]. Wavy collagen fiber bundles necessitate time for uncrimping and reorienting to straighten enough before being able to withstand the applied stress causing a lower dynamic modulus compared to when thin fibers are more organized and densely packed. Furthermore, an in vitro study has previously shown how collagen microstructure affects strain transmission and the overall viscoelastic behavior of the tissue [55]. When collagen is locally oriented perpendicular to the loading direction, the structure cannot support the tensile load at high strain values causing some local micro-failure to occur by buckling. A similar scenario may occur in UL tendons in specific regions where fibers are extremely crimped. When abrupt and substantial changes in fiber orientation occur, the fibers can be, in small areas, almost perpendicular to the main tendon axes. This exemplifies how the local architecture of the fibers, as crimp, can impact the tendon mechanical response. Moreover, when fibers are more crimped and less homogeneously aligned as in UL tendons, they are also less efficiently packed (expressed in this study as lower fiber density) which can further hinder fiber recruitment. Additionally, the difference in structural organization between UL and FL tendons may affect the extent of sliding of fibers and fibrils, as well as the ability of fibrils to reorganize within the fibers. However, at the fibrillar level no substantial differences in fibril order were observed. In UL tendons, fibrils exhibited a delayed mechanical response but, after the initial phase, presented a similar behavior to FL tendons. Although fibril strain relaxation ratios were increased and fibril relaxation time was faster in UL than in FL tendons, the relationship between tissue to fibril level remained similar between the two groups. Consequently, the differences in mechanical response between UL and FL tendons are most likely not due to inherently different fibril properties but are instead most likely translated from other length scales. However, interestingly, our in situ data showed that the relaxation of the fibrils is 10–20% slower than the relaxation at the organ level. This is possibly due to the strain partitioning through hierarchical levels [56,57]. Previous mechanical studies on isolated fibrils revealed that, when extracted from the matrix, fibrils relax

faster than the whole organ [57,58]. However, fibrils are functionally discontinuous within the tendon tissue, which allows them to stretch and slide. Thereby the applied load is partitioned between different structural levels [36,48,59].

Recently more and more studies have been showing the importance of computational approaches to better understand the complex tendon biomechanics [32,60–62]. Experimental data from all tendon hierarchical levels that consider the interactions occurring between different length scales are needed to validate these computational models. Thus, the results presented in our study could be beneficial in the future to tune parameters necessary for material modeling [63,64].

4.3. Compositional differences in tendon tissue due to reduced loading

The extracellular matrix protein elastin dominates the mechanical response of highly flexible collagenous tissues like the heart valve, arteries and some ligaments [65–67]. Recent studies have shown that elastin also plays a role in tendon mechanical properties [68,69]. Elastin mainly contributes to the tissue mechanical behavior in the toe region of the stress–strain curve, and it can also contribute to load support in the linear region [70]. In fact, elastin stabilizes the crimp wave-pattern at low strains easing the recruitment of fibers during the passage to the linear region of the stress–strain curve [71]. Consequently, elastin may help to prevent micro-structural failure during loading. Moreover, in the aortic valve leaflet elastin helps collagen fibers to return to their specific configuration between successive loading cycles, and it is thus critical to maintain functional tissues that are cyclically loaded [72]. Our results indicate that in tendons elastin content may slightly decrease as a consequence of reduced loading. In turn, this could cause a reduction in interfibrillar sliding and destabilizing the crimp-pattern at low strains in UL tendons contributing to the biomechanical differences observed between UL and FL tendons. As in this study the tendons were exposed to reduced loading for 4 weeks, it would be of interest in the future to investigate if a longer unloading would decrease elastin content further.

Interestingly, our results show that cell density is significantly reduced in UL compared to FL tendons. A decrease of tendon cells may over time lead to macroscopic alterations in composition and structure of the tissue, leading to altered mechanical properties [73,74]. Therefore, a longer period of reduced loading would also be of interest for future studies, as the effect of the cell reduction on extracellular matrix composition and structure may take longer to fully occur.

Another important part for tendon structure and function is collagen cross linking which was not investigated here. Cross links are essential in preventing sliding by tying collagen triple helixes to each other [8,75]. A reduced level of cross-links in tendon tissue could also be associated with reduced loading and altered mechanical properties, which can be of interest for future research.

Although collagen is the main load-bearing component in tendons, non-collagenous proteins also play a part in tendon mechanics by affecting the bonding between fibrils [76]. Proteoglycans are fundamental constituents of the extracellular matrix performing different mechanical functions, e.g. transmitting tensile loads like decorin [77], or altering compressive stress, like aggrecans [78]. In tendons, proteoglycans, being substantially less stiff than the fibrils, can transfer some of the shear stress [78]. Even if this study did not reveal differences in proteoglycan content between UL and FL tendons, future studies may show a connection between unloading and other extracellular matrix proteins.

Furthermore, manual measurements of the cross-sectional area (CSA), indicted that UL tendons have 40–60% larger CSA compared to FL tendons (Supporting Information, Table S1). This could be associated with an increase in water content, because of the less effective fiber packing in UL tendons due to crimping. However, measurements of CSA in SR-PhC-μCT images only showed a 10% increase in UL vs FL loaded tendons (Supporting Information, Figure S10). The tomograms showed an increased presence of adipose deposits and other tissues surrounding the UL tendons (Supporting Information, Figure S10), which were most likely included in the manual measurements and could explain the differences between the two measurements. This observation further underlines the power and importance of using high resolution 3D imaging to accurately determine structural properties and elucidate the observed differences in mechanical response. However, to avoid radiation induced damage, tendons mechanically probed in this study were not imaged before the test. Therefore, the calculations for mechanical properties still rely on manual CSA measurements, which can be seen as a limitation.

4.4. Local variability of the intra-tendon structure

Computational studies have demonstrated that deformations within Achilles tendons are region specific and closely linked to variations in mechanical properties between the proximal (muscle side) and distal (bone side) tendon [79]. In the proximal region, stress is ∼70% lower and stiffness is ∼30% lower than in the inferior portion of the Achilles tendon [79]. In turn, these region-specific variations in mechanical properties could be reconducted to structural and conformational differences. In human Achilles tendons, fascicles close to the muscles can twist and, thereby redistributing stress within the tissue [80]. In rat tendons, fascicles are not distinguishable. However, the 3 sub-tendons separate close to the muscles allowing for more effective twisting, as observed during the ex situ mechanical tests in this study. The twisting allows strain concentrations in the tendon to be redistributed to wider areas, leading to higher effective tissue strength [80]. Our results show that close to the tendon-muscle junction, fibers were more crimped in both UL and FL tendons. The reason for this could be that at the tendon-muscle junction, the fibers become extremely rippled to effectively intercalate with the muscles (Supporting Information, Figure S9). Longitudinal differences in structure and mechanical properties may allow the muscle junction portion of the tendon to function as a mechanical buffer to protect the stiffer lower portion of the Achilles tendon from injury. However, in FL tendons there is a clear distinction between the structural order in the center and close to the muscles, whereas in the UL tendons fiber organization is more similar between the two regions.

We have also shown that SOL fibers are significantly less oriented than MG and LG fibers. Mechanical differences between the SOL sub-tendon and the other two sub-tendons have previously been observed, showing that the SOL strains almost twice as much as MG and LG when all muscles are stimulated simultaneously [81,82]. Furthermore, the anterior part of the Achilles tendon, where the SOL is located, elongates and strains more than the posterior part, where MG and LG are located [81,82]. Our results indicate that the higher levels of crimping in the SOL could be the reason why this sub-tendon can sustain higher strain compared to MG and LG sub-tendons [83,84]. Additionally, previous studies have suggested that heterogeneous loading within the tendon leads to non-uniform stress distribution, which causes tendons to be more prone to injury [85]. Therefore, further investigations of these aspects could be of great interest. The use of synchrotron X-ray tomography in combination with in situ mechanical loading and digital volume correlation [86–88] could represent a successful approach to elucidate the complex relation between local tissue strains, the specific microstructure in Achilles sub-tendons and in vivo loading regimes.

5. Conclusions

Lack of physiological mechanical loading can have detrimental effects on tendon structure and mechanical properties. This multiscale and multimodal study provides new insights about the relation between in vivo loading, the Achilles tendon nano- to meso– structure and tendon mechanical properties. For the first time, we have visualized and explained where the altered mechanical response originates from. We have shown that structural properties, such as orientation, are transmitted through hierarchical levels, and that structural inhomogeneity at the fiber-level, caused by reduced in vivo loading, impairs the viscoelastic properties of the Achilles tendon. Additionally, reduced loading decreases cell density which could impair the turnover capacity in the tissue and thus the structure and composition and mechanical properties of the tendon. The results provide novel understanding of the mechano-regulatory mechanisms that regulate the structural organization and biomechanics of a complex collagen-based tissue. In the future, these findings might help to design tailored rehabilitation protocols, after a period of immobilization, to better regain performance for tendons or other collagen-based tissues.

Declaration of Competing Interest

The authors have no financial/commercial Conflict of Interest.

CRediT authorship contribution statement

Maria Pierantoni: Investigation, Methodology, Formal analysis, Validation, Writing – original draft. **Isabella Silva Barreto:** Investigation, Methodology, Formal analysis, Validation, Writing – original draft. **Malin Hammerman:** Data curation, Methodology, Investigation, Validation, Writing – review & editing. **Vladimir Novak:** Methodology, Resources, Writing – review & editing. **Ana Diaz:** Data curation, Methodology, Resources, Writing – review & editing. **Jonas Engqvist:** Methodology, Writing – review & editing. **Pernilla Eliasson:** Conceptualization, Data curation, Investigation, Funding acquisition, Supervision, Writing – review & editing. **Hanna Isaksson:** Conceptualization, Data curation, Investigation, Funding acquisition, Supervision, Writing – review & editing.

Acknowledgments

Funding from the Knut and Alice Wallenberg KAW Foundation (Wallenberg Academy Fellows 2017.0221) and the European Research Council (ERC) under the European Union's Horizon 2020 research and innovation program (grant agreement No 101002516), the Royal Physiographic Society of Lund (41380), the Greta and Johan Kocks foundation, the Swedish Research Council (VR2017–00990), the Swedish National centre for Research in Sports (P2021–0032), Magnus Bergvall foundation (2019–03211) and Åke Wiberg foundation (M20–0021) are greatly acknowledged. VN acknowledges funding from the European Union's Horizon 2020 research and innovation program under the Marie Skłodowska-Curie Grant Agreement No 701647. We acknowledge the European Union's Horizon 2020 research and innovation program under grant agreement No 731019 (EUSMI), which provided beamtime at the cSAXS beamline. We acknowledge the Paul Scherrer Institut, Villigen, Switzerland for provision of synchrotron radiation beamtime at the TOMCAT beamline X02DA and at the cSAXS beamline X12SA of the SLS. We acknowledge the Core Facility Microscopy Unit at Linköping University for the use of Lecia DMi8 microscope.

Supplementary materials

Supplementary material associated with this article can be found, in the online version, at doi:10.1016/j.actbio.2023.07.021.

References

[1] C. Stecco, W. Hammer, A. Vleeming, R. De Caro, 1 - Connective tissues, in: C. Stecco, W. Hammer, A. Vleeming, R. De Caro (Eds.), Funct. Atlas Hum. Fascial Syst., Churchill Livingstone, 2015, pp. 1–20, doi:10.1016/B978-0-7020-4430-4.00001-4.
[2] P. Kannus, Structure of the tendon connective tissue, Scand, J. Med. Sci. Sports. 10 (2000) 312–320, doi:10.1034/j.1600-0838.2000.010006312.x.
[3] P.P. Provenzano, R. Vanderby, Collagen fibril morphology and organization: implications for force transmission in ligament and tendon, Matrix Biol. 25 (2006) 71–84, doi:10.1016/j.matbio.2005.09.005.
[4] J.H.-C. Wang, Mechanobiology of tendon, J. Biomech. 39 (2006) 1563–1582, doi:10.1016/j.jbiomech.2005.05.011.
[5] T. Thorpe Chavaunne, P. Udeze Chineye, L. Birch Helen, D. Clegg Peter, R.C. Screen Hazel, Specialization of tendon mechanical properties results from interfascicular differences, J. R. Soc. Interface 9 (2012) 3108–3117, doi:10.1098/rsif.2012.0362.
[6] C.T. Thorpe, C. Klemt, G.P. Riley, H.L. Birch, P.D. Clegg, H.R.C. Screen, Helical sub-structures in energy-storing tendons provide a possible mechanism for efficient energy storage and return, Acta Biomater. 9 (2013) 7948–7956, doi:10.1016/j.actbio.2013.05.004.
[7] N. Maffulli, P. Sharma, K.L. Luscombe, Achilles tendinopathy: aetiology and management, J. R. Soc. Med. 97 (2004) 472–476.
[8] K.M. Heinemeier, M. Kjaer, In vivo investigation of tendon responses to mechanical loading, J. Musculoskelet. Neuronal Interact. 11 (2011) 115–123.
[9] J.H.-C. Wang, Q. Guo, B. Li, Tendon biomechanics and mechanobiology—a minireview of basic concepts and recent advancements, J. Hand Ther. 25 (2012) 133–141, doi:10.1016/j.jht.2011.07.004.
[10] H. Khayyeri, P. Blomgran, M. Hammerman, M.J. Turunen, A. Löwgren, M. Guizar-Sicairos, P. Aspenberg, H. Isaksson, Achilles tendon compositional and structural properties are altered after unloading by botox, Sci. Rep. 7 (2017) 13067, doi:10.1038/s41598-017-13107-7.
[11] M.D. De Boer, A. Selby, P. Atherton, K. Smith, O.R. Seynnes, C.N. Maganaris, N. Maffulli, T. Movin, M.V. Narici, M.J. Rennie, The temporal responses of protein synthesis, gene expression and cell signalling in human quadriceps muscle and patellar tendon to disuse, J. Physiol. 585 (2007) 241–251, doi:10.1113/jphysiol.2007.142828.
[12] K. Dideriksen, A.P. Boesen, S. Reitelseder, C. Couppé, R. Svensson, P. Schjerling, S.P. Magnusson, L. Holm, M. Kjaer, Tendon collagen synthesis declines with immobilization in elderly humans: no effect of anti-inflammatory medication, J. Appl. Physiol. 122 (2017) 273–282, doi:10.1152/japplphysiol.00809.2015.
[13] P. Blomgran, R. Blomgran, J. Ernerudh, P. Aspenberg, A possible link between loading, inflammation and healing: immune cell populations during tendon healing in the rat, Sci. Rep. 6 (2016) 29824, doi:10.1038/srep29824.
[14] G. Yang, H.-J. Im, J.H.-C. Wang, Repetitive mechanical stretching modulates IL-1β induced COX-2, MMP-1 expression, and PGE2 production in human patellar tendon fibroblasts, Gene 363 (2005) 166–172, doi:10.1016/j.gene.2005.08.006.
[15] K. Kubo, H. Akima, J. Ushiyama, I. Tabata, H. Fukuoka, H. Kanehisa, T. Fukunaga, Effects of 20 days of bed rest on the viscoelastic properties of tendon structures in lower limb muscles, Br. J. Sports Med. 38 (2004) 324–330, doi:10.1136/bjsm.2003.005595.
[16] N.D. Reeves, C.N. Maganaris, G. Ferretti, M.V. Narici, Influence of 90-day simulated microgravity on human tendon mechanical properties and the effect of resistive countermeasures, J. Appl. Physiol. 98 (2005) 2278–2286, doi:10.1152/japplphysiol.01266.2004.
[17] C.N. Maganaris, N.D. Reeves, J. Rittweger, A.J. Sargeant, D.A. Jones, K. Gerrits, A. De Haan, Adaptive response of human tendon to paralysis, Muscle Nerve 33 (2006) 85–92, doi:10.1002/mus.20441.
[18] U.G. Longo, M. Ronga, N. Maffulli, Acute ruptures of the Achilles tendon, Sports Med. Arthrosc. Rev. 17 (2009) 127–138, doi:10.1097/JSA.0b013e3181a3d767.
[19] G.W. Hess, Achilles tendon rupture: a review of etiology, population, anatomy, risk factors, and injury prevention, Foot Ankle Spec 3 (2010) 29–32, doi:10.1177/1938640009355191.
[20] J. Leppilahti, J. Puranen, S. Orava, Incidence of Achilles tendon rupture, Acta Orthop. Scand. 67 (1996) 277–279, doi:10.3109/17453679608994688.
[21] M. Lavagnino, M.E. Wall, D. Little, A.J. Banes, F. Guilak, S.P. Arnoczky, Tendon mechanobiology: current knowledge and future research opportunities, J. Orthop. Res. Off. Publ. Orthop. Res. Soc. 33 (2015) 813–822, doi:10.1002/jor.22871.
[22] A. Wilson, G. Lichtwark, The anatomical arrangement of muscle and tendon enhances limb versatility and locomotor performance, Philos. Trans. R. Soc. B 366 (2011) 1540–1553, doi:10.1098/rstb.2010.0361.
[23] P.V. Komi, S. Fukashiro, M. Järvinen, Biomechanical loading of Achilles tendon during normal locomotion, Clin. Sports Med. 11 (1992) 521–531.
[24] G.G. Handsfield, L.C. Slane, H.R.C. Screen, Nomenclature of the tendon hierarchy: an overview of inconsistent terminology and a proposed size-based naming scheme with terminology for multi-muscle tendons, J. Biomech. 49 (2016) 3122–3124, doi:10.1016/j.jbiomech.2016.06.028.
[25] F. Klatte-Schulz, S. Minkwitz, A. Schmock, N. Bormann, A. Kurtoglu, S. Tsitsilonis, S. Manegold, B. Wildemann, Different Achilles tendon pathologies show

distinct histological and molecular characteristics, Int. J. Mol. Sci. 19 (2018), doi:10.3390/ijms19020404.
[26] D. Laudier, M.B. Schaffler, E.L. Flatow, V.M. Wang, Novel procedure for high-fidelity tendon histology, J. Orthop. Res. 25 (2007) 390–395, doi:10.1002/jor.20304.
[27] M. Pierantoni, I. Silva Barreto, M. Hammerman, L. Verhoeven, E. Törnquist, V. Novak, R. Mokso, P. Eliasson, H. Isaksson, A quality optimization approach to image Achilles tendon microstructure by phase-contrast enhanced synchrotron micro-tomography, Sci. Rep. 11 (2021) 1–14, doi:10.1038/s41598-021-96589-w.
[28] Y. Zhou, J. Hu, J. Zhou, Z. Zeng, Y. Cao, Z. Wang, C. Chen, C. Zheng, H. Chen, H. Lu, Three-dimensional characterization of the microstructure in rabbit patella–patellar tendon interface using propagation phase-contrast synchrotron radiation microtomography, J. Synchrotron Radiat. 25 (2018) 1833–1840, doi:10.1107/S160057751801353X.
[29] T. Zhang, S. Li, Y. Chen, H. Xiao, L. Wang, J. Hu, D. Xu, H. Lu, Characterize the microstructure change after tendon enthesis injury using synchrotron radiation μCT, J. Orthop. Res. 40 (2022) 2678–2687, doi:10.1002/jor.25289.
[30] P. Fratzl, Collagen: structure and mechanics, an introduction, in: P. Fratzl (Ed.), Collagen Struct. Mech., Springer US, Boston, MA, 2008, pp. 1–13, doi:10.1007/978-0-387-73906-9_1.
[31] M.J. Turunen, H. Khayyeri, M. Guizar-Sicairos, H. Isaksson, Effects of tissue fixation and dehydration on tendon collagen nanostructure, J. Struct. Biol. 199 (2017) 209–215, doi:10.1016/j.jsb.2017.07.009.
[32] A. Gautieri, F.S. Passini, U. Silván, M. Guizar-Sicairos, G. Carimati, P. Volpi, M. Moretti, H. Schoenhuber, A. Redaelli, M. Berli, J.G. Snedeker, Advanced glycation end-products: mechanics of aged collagen from molecule to tissue, Matrix Biol. 59 (2017) 95–108, doi:10.1016/j.matbio.2016.09.001.
[33] S.R. Inamdar, S. Prévost, N.J. Terrill, M.M. Knight, H.S. Gupta, Reversible changes in the 3D collagen fibril architecture during cyclic loading of healthy and degraded cartilage, Acta Biomater. 136 (2021) 314–326, doi:10.1016/j.actbio.2021.09.037.
[34] I. Silva Barreto, M. Pierantoni, M. Hammerman, E. Törnquist, S.L. Cann, A. Diaz, J. Engqvist, M. Liebi, P. Eliasson, H. Isaksson, Nanoscale characterization of collagen structural responses to *in situ* loading in rat Achilles tendons, Matrix Biol. 115 (2023) 32–47, doi:10.1016/j.matbio.2022.11.006.
[35] A. Gustafsson, N. Mathavan, M.J. Turunen, J. Engqvist, H. Khayyeri, S.A. Hall, H. Isaksson, Linking multiscale deformation to microstructure in cortical bone using in situ loading, digital image correlation and synchrotron X-ray scattering, Acta Biomater. 69 (2018) 323–331, doi:10.1016/j.actbio.2018.01.037.
[36] G. Fessel, Y. Li, V. Diederich, M. Guizar-Sicairos, P. Schneider, D.R. Sell, V.M. Monnier, J.G. Snedeker, Advanced glycation end-products reduce collagen molecular sliding to affect collagen fibril damage mechanisms but not stiffness, PLoS ONE 9 (2014) e110948, doi:10.1371/journal.pone.0110948.
[37] M. Hammerman, F. Dietrich-Zagonel, P. Blomgran, P. Eliasson, P. Aspenberg, Different mechanisms activated by mild versus strong loading in rat Achilles tendon healing, PLoS ONE 13 (2018) e0201211, doi:10.1371/journal.pone.0201211.
[38] J.V. Cichon Jr., T.V. Mccaffrey, W.J. Litchy, J.L. Knops, The effect of botulinum toxin type a injection on compound muscle action potential in an in vivo rat model, The Laryngoscope. 105 (1995) 144–148. 10.1288/00005537-199502000-00006.
[39] S.L. Manske, S.K. Boyd, R.F. Zernicke, Vertical ground reaction forces diminish in mice after botulinum toxin injection, J. Biomech. 44 (2011) 637–643, doi:10.1016/j.jbiomech.2010.11.011.
[40] F. Dietrich-Zagonel, M. Hammerman, M. Bernhardsson, P. Eliasson, Effect of storage and preconditioning of healing rat Achilles tendon on structural and mechanical properties, Sci. Rep. 11 (2021) 958, doi:10.1038/s41598-020-80299-w.
[41] A.H. Lee, D.M. Elliott, Freezing does not alter multiscale tendon mechanics and damage mechanisms in tension, Ann. N. Y. Acad. Sci. 1409 (2017) 85–94, doi:10.1111/nyas.13460.
[42] N.P. Quirk, C. Lopez De Padilla, R.E. De La Vega, M.J. Coenen, A. Tovar, C.H. Evans, S.A. Müller, Effects of freeze-thaw on the biomechanical and structural properties of the rat Achilles tendon, J. Biomech. 81 (2018) 52–57, doi:10.1016/j.jbiomech.2018.09.012.
[43] M. Stampanoni, A. Groso, A. Isenegger, G. Mikuljan, Q. Chen, A. Bertrand, S. Henein, R. Betemps, U. Frommherz, P. Böhler, D. Meister, M. Lange, R. Abela, Trends in synchrotron-based tomographic imaging: the SLS experience, Dev. X-Ray Tomogr. V, SPIE, 6318, 2006, pp. 193–206, doi:10.1117/12.679497.
[44] C.T. Rueden, J. Schindelin, M.C. Hiner, B.E. DeZonia, A.E. Walter, E.T. Arena, K.W. Eliceiri, ImageJ2: imageJ for the next generation of scientific image data, BMC Bioinformatics 18 (2017) 529, doi:10.1186/s12859-017-1934-z.
[45] Dragonfly 4.6 Object Research Systems (ORS) Inc, Montreal, Canada, 2018; software. http://www.theobjects.com/dragonfly.
[46] M. Krause, J.M. Hausherr, B. Burgeth, C. Herrmann, W. Krenkel, Determination of the fibre orientation in composites using the structure tensor and local X-ray transform, J. Mater. Sci. 45 (2010) 888–896, doi:10.1007/s10853-009-4016-4.
[47] P. Saxena, G. Bissacco, C. Gundlach, V.A. Dahl, C.H. Trinderup, A.B. Dahl, Process characterization for molding of paper bottles using computed tomographyand structure tensor analysis, J. Nondestruct. Test. Ultrasound. 445 (2019) 3.
[48] I. Silva Barreto, M. Pierantoni, M. Hammerman, E. Törnquist, S.L. Cann, A. Diaz, J. Engqvist, M. Liebi, P. Eliasson, H. Isaksson, Nanoscale characterization of collagen structural responses to in situ loading in rat achilles tendons, Matrix Biol. 115 (2023) 32–47, doi:10.1016/j.matbio.2022.11.006.
[49] M.W. Hast, A. Zuskov, L.J. Soslowsky, The role of animal models in tendon research, Bone Jt. Res. 3 (2014) 193–202, doi:10.1302/2046-3758.36.2000281.
[50] D. Shin, T. Finni, S. Ahn, J.A. Hodgson, H.-D. Lee, V.R. Edgerton, S. Sinha, Effect of chronic unloading and rehabilitation on human Achilles tendon properties: a velocity-encoded phase-contrast MRI study, J. Appl. Physiol. 105 (2008) 1179–1186, doi:10.1152/japplphysiol.90699.2008.
[51] J.H. Shepherd, G.P. Riley, H.R.C. Screen, Early stage fatigue damage occurs in bovine tendon fascicles in the absence of changes in mechanics at either the gross or micro-structural level, J. Mech. Behav. Biomed. Mater. 38 (2014) 163–172, doi:10.1016/j.jmbbm.2014.06.005.
[52] V.W.T. Cheng, H.R.C. Screen, The micro-structural strain response of tendon, J. Mater. Sci. 42 (2007) 8957–8965, doi:10.1007/s10853-007-1653-3.
[53] H.R.C. Screen, D.A. Lee, D.L. Bader, J.C. Shelton, Development of a technique to determine strains in tendons using the cell nuclei, Biorheology 40 (2003) 361–368.
[54] M. Ventre, F. Mollica, P.A. Netti, The effect of composition and microstructure on the viscoelastic properties of dermis, J. Biomech. 42 (2009) 430–435, doi:10.1016/j.jbiomech.2008.12.004.
[55] B.A. Roeder, K. Kokini, S.L. Voytik-Harbin, Fibril microstructure affects strain transmission within collagen extracellular matrices, J. Biomech. Eng. 131 (2009) 031015, doi:10.1115/1.3005331.
[56] C.T. Thorpe, M.S.C. Godinho, G.P. Riley, H.L. Birch, P.D. Clegg, H.R.C. Screen, The interfascicular matrix enables fascicle sliding and recovery in tendon, and behaves more elastically in energy storing tendons, J. Mech. Behav. Biomed. Mater. 52 (2015) 85–94, doi:10.1016/j.jmbbm.2015.04.009.
[57] B.E. Peterson, S.E. Szczesny, Dependence of tendon multiscale mechanics on sample gauge length is consistent with discontinuous collagen fibrils, Acta Biomater. 117 (2020) 302–309, doi:10.1016/j.actbio.2020.09.046.
[58] H.R.C. Screen, Investigating load relaxation mechanics in tendon, J. Mech. Behav. Biomed. Mater. 1 (2008) 51–58, doi:10.1016/j.jmbbm.2007.03.002.
[59] N. Sasaki, S. Odajima, Elongation mechanism of collagen fibrils and force-strain relations of tendon at each level of structural hierarchy, J. Biomech. 29 (1996) 1131–1136, doi:10.1016/0021-9290(96)00024-3.
[60] N. Karathanasopoulos, G. Arampatzis, J.-F. Ganghoffer, Unravelling the viscoelastic, buffer-like mechanical behavior of tendons: a numerical quantitative study at the fibril-fiber scale, J. Mech. Behav. Biomed. Mater. 90 (2019) 256–263, doi:10.1016/j.jmbbm.2018.10.019.
[61] N. Karathanasopoulos, P. Angelikopoulos, C. Papadimitriou, P. Koumoutsakos, Bayesian identification of the tendon fascicle's structural composition using finite element models for helical geometries, Comput. Methods Appl. Mech. Eng. 313 (2017) 744–758, doi:10.1016/j.cma.2016.10.024.
[62] H. Chen, X. Zhao, X. Lu, G. Kassab, Non-linear micromechanics of soft tissues, Int. J. Non-Linear Mech. 56 (2013) 79–85, doi:10.1016/j.ijnonlinmec.2013.03.002.
[63] T. Notermans, H. Khayyeri, H. Isaksson, Understanding how reduced loading affects Achilles tendon mechanical properties using a fibre-reinforced poro-visco-hyper-elastic model, J. Mech. Behav. Biomed. Mater. 96 (2019) 301–309, doi:10.1016/j.jmbbm.2019.04.041.
[64] H. Khayyeri, A. Gustafsson, A. Heuijerjans, M.K. Matikainen, P. Julkunen, P. Eliasson, P. Aspenberg, H. Isaksson, A fibre-reinforced poroviscoelastic model accurately describes the biomechanical behaviour of the rat Achilles tendon, PLoS ONE 10 (2015) e0126869, doi:10.1371/journal.pone.0126869.
[65] T.C. Lee, R.J. Midura, V.C. Hascall, I. Vesely, The effect of elastin damage on the mechanics of the aortic valve, J. Biomech. 34 (2001) 203–210, doi:10.1016/S0021-9290(00)00187-1.
[66] A.J. Cocciolone, J.Z. Hawes, M.C. Staiculescu, E.O. Johnson, M. Murshed, J.E. Wagenseil, Elastin, arterial mechanics, and cardiovascular disease, Am. J. Physiol. Heart Circ. Physiol. 315 (2018) H189–H205, doi:10.1152/ajpheart.00087.2018.
[67] H.B. Henninger, W.R. Valdez, S.A. Scott, J.A. Weiss, Elastin governs the mechanical response of medial collateral ligament under shear and transverse tensile loading, Acta Biomater 25 (2015) 304–312, doi:10.1016/j.actbio.2015.07.011.
[68] F. Fang, S.P. Lake, Multiscale mechanical integrity of human supraspinatus tendon in shear after elastin depletion, J. Mech. Behav. Biomed. Mater. 63 (2016) 443–455, doi:10.1016/j.jmbbm.2016.06.032.
[69] J.D. Eekhoff, F. Fang, L.G. Kahan, G. Espinosa, A.J. Cocciolone, J.E. Wagenseil, R.P. Mecham, S.P. Lake, Functionally distinct tendons from elastin haploinsufficient mice exhibit mild stiffening and tendon-specific structural alteration, J. Biomech. Eng. 139 (2017) 111003, doi:10.1115/1.4037932.
[70] K.A. Hansen, J.A. Weiss, J.K. Barton, Recruitment of tendon crimp with applied tensile strain, J. Biomech. Eng. 124 (2001) 72–77, doi:10.1115/1.1427698.
[71] H.B. Henninger, C.J. Underwood, S.J. Romney, G.L. Davis, J.A. Weiss, Effect of elastin digestion on the quasi-static tensile response of medial collateral ligament, J. Orthop. Res. 31 (2013) 1226–1233, doi:10.1002/jor.22352.
[72] I. Vesely, The role of elastin in aortic valve mechanics, J. Biomech. 31 (1997) 115–123, doi:10.1016/S0021-9290(97)00122-X.
[73] C.M. Nelson, R.P. Jean, J.L. Tan, W.F. Liu, N.J. Sniadecki, A.A. Spector, C.S. Chen, Emergent patterns of growth controlled by multicellular form and mechanics, Proc. Natl. Acad. Sci. 102 (2005) 11594–11599, doi:10.1073/pnas.0502575102.
[74] B.I. Shraiman, Mechanical feedback as a possible regulator of tissue growth, Proc. Natl. Acad. Sci. 102 (2005) 3318–3323, doi:10.1073/pnas.0404782102.
[75] B.G. Godard, C.-P. Heisenberg, Cell division and tissue mechanics, Curr. Opin. Cell Biol. 60 (2019) 114–120, doi:10.1016/j.ceb.2019.05.007.
[76] J.E. Scott, Elasticity in extracellular matrix "shape modules" of tendon, cartilage, etc. A sliding proteoglycan-filament model, J. Physiol. 553 (2003) 335–343, doi:10.1113/jphysiol.2003.050179.

[77] D.M. Elliott, P.S. Robinson, J.A. Gimbel, J.J. Sarver, J.A. Abboud, R.V. Iozzo, L.J. Soslowsky, Effect of altered matrix proteins on quasilinear viscoelastic properties in transgenic mouse tail tendons, Ann. Biomed. Eng. 31 (2003) 599–605, doi:10.1114/1.1567282.
[78] P. Fratzl, I. Burgert, H.S. Gupta, On the role of interface polymers for the mechanics of natural polymeric composites, Phys. Chem. Chem. Phys. 6 (2004) 5575–5579, doi:10.1039/B411986J.
[79] N.D. Reeves, G. Cooper, Is human Achilles tendon deformation greater in regions where cross-sectional area is smaller? J. Exp. Biol. 220 (2017) 1634–1642, doi:10.1242/jeb.157289.
[80] V.B. Shim, G.G. Handsfield, J.W. Fernandez, D.G. Lloyd, T.F. Besier, Combining in silico and in vitro experiments to characterize the role of fascicle twist in the Achilles tendon, Sci. Rep. 8 (2018) 13856, doi:10.1038/s41598-018-31587-z.
[81] S.J. Obst, R. Newsham-West, R.S. Barrett, Changes in Achilles tendon mechanical properties following eccentric heel drop exercise are specific to the free tendon, Scand. J. Med. Sci. Sports. 26 (2016) 421–431, doi:10.1111/sms.12466.
[82] G.A. Lichtwark, A.G. Cresswell, R.J. Newsham-West, Effects of running on human Achilles tendon length-tension properties in the free and gastrocnemius components, J. Exp. Biol. 216 (2013) 4388–4394, doi:10.1242/jeb.094219.
[83] T. Finni, M. Bernabei, G.C. Baan, W. Noort, C. Tijs, H. Maas, Non-uniform displacement and strain between the soleus and gastrocnemius subtendons of rat Achilles tendon, Scand, J. Med. Sci. Sports 28 (2018) 1009–1017, doi:10.1111/sms.13001.
[84] A. Arndt, A.-S. Bengtsson, M. Peolsson, A. Thorstensson, T. Movin, Non-uniform displacement within the Achilles tendon during passive ankle joint motion, Knee Surg. Sports Traumatol. Arthrosc. 20 (2012) 1868–1874, doi:10.1007/s00167-011-1801-9.
[85] J. Bojsen-Møller, S.P. Magnusson, Heterogeneous loading of the human Achilles tendon in vivo, Exerc. Sport Sci. Rev. 43 (2015) 190–197, doi:10.1249/JES.0000000000000062.
[86] M. Peña Fernández, A.P. Kao, R. Bonithon, D. Howells, A.J. Bodey, K. Wanelik, F. Witte, R. Johnston, H. Arora, G. Tozzi, Time-resolved in situ synchrotron-microCT: 4D deformation of bone and bone analogues using digital volume correlation, Acta Biomater. 131 (2021) 424–439, doi:10.1016/j.actbio.2021.06.014.
[87] C.M. Disney, A. Eckersley, J.C. McConnell, H. Geng, A.J. Bodey, J.A. Hoyland, P.D. Lee, M.J. Sherratt, B.K. Bay, Synchrotron tomography of intervertebral disc deformation quantified by digital volume correlation reveals microstructural influence on strain patterns, Acta Biomater. 92 (2019) 290–304, doi:10.1016/j.actbio.2019.05.021.
[88] K. Madi, K.A. Staines, B.K. Bay, B. Javaheri, H. Geng, A.J. Bodey, S. Cartmell, A.A. Pitsillides, P.D. Lee, In situ characterization of nanoscale strains in loaded whole joints via synchrotron X-ray tomography, Nat. Biomed. Eng. 4 (2020) 343–354, doi:10.1038/s41551-019-0477-1.